European Journal of Chemistry
Journal homepage: www.eurjchem.com

Geometrical, electronic structure, nonlinear optical and spectroscopic investigations of 4-(phenylthio)phthalonitrile dye sensitizer for solar cells using quantum chemical calculations

Ponnusamy Munusamy Anbarasan*, Palanivel Senthil Kumar, Kolandan Vasudevan, Raji Govindan, Annamalai Prakasam and Munusamy Geetha

Department of Physics, Periyar University, Salem-636 011, Tamilnadu, India

**Corresponding author at: Department of Physics, Periyar University, Salem-636 011, Tamilnadu, India. Tel.: +91.0427.2345766; fax: +91.0427.2345565.*
E-mail address: anbarasanpm@gmail.com (P.M. Anbarasan).

ARTICLE INFORMATION

Received: 02 September 2010
Received in revised form: 26 January 2011
Accepted: 15 February 2011
Online: 30 June 2011

KEYWORDS

Dye Sensitizer
Density Functional Theory
Electronic Structure
NBO Analysis
Absorption Spectrum
n → π* Transitions

ABSTRACT

The geometries, electronic structures, polarizabilities, and hyperpolarizabilities of organic dye sensitizer 4-(phenylthio)phthalonitrile were studied based on Density Functional Theory (DFT) using the hybrid functional B3LYP. Ultraviolet-Visible (UV-Vis) spectrum was investigated by using a hybrid method which combines CIS-DFT (B3LYP). The absorption bands are assigned to n→π* transitions. The results were showed 4-(phenylthio) phthalonitrile used in Dye Sensitized Solar Cells (DSSC) give a good conversion efficiency.

1. Introduction

The new technologies for direct solar energy conversion have gained more attention in the last few years. In particular, dye sensitized solar cells (DSSCs) are promising in terms of efficiency and low cost [1-3]. The leading feature of DSSC consists in a wide band gap nanocrystalline film grafted with a quasi-monolayer of dye molecules and submerged in a redox electrolyte. This elegant architecture can synchronously address two critical issues of employing organic materials for the photovoltaic applications: (*i*) efficient charge generation from the Frenkel excitons and (*ii*) long-lived electron-hole separation up to the millisecond time domain. The latter attribute can often confer an almost quantitative charge collection for several micrometer-thick active layers, even if the electron mobilities in nanostructured semiconducting films are significantly lower than those in the bulk crystalline materials. Benefited from systematic device engineering and continuous material innovation, a state of the art DSSC with a ruthenium sensitizer has achieved a validated efficiency of 11.1% [4] measured under the air mass 1.5 global (AM1.5G) conditions. In view of the limited ruthenium resource and the heavy-metal toxicity, metal-free organic dyes have received surging research interest in recent years [5-21]. Because of their high molar absorption coefficient, relatively simple synthesis procedure, various structures and lower cost in contrast to a ruthenium dye and the flexibility in molecular tailoring of an organic sensitizer provides a large area to explore [22-24]. Moreover, recently a rapid progress of organic dyes has been witnessed reaching close to 10.0% efficiencies in combination with a volatile acetonitrile-based electrolyte [25]. Phthalo nitrile is an important class of high performance dyes, which are easily processable, and display good mechanical properties, outstanding thermal and thermal-oxidative stability. Phthalonitrile dyes were used for aerospace, marine, and electronic packaging applications. By thermal treatment of phthalonitrile derivatives at elevated temperatures (generally high up to 350 °C) for an extended period of time, Filippo *et al*. reported that nitrile or cyanide (CN) group also good anchoring with the surface of the nanocrystal TiO_2 particles and provide good electron transfer channel [26]. In this paper the performance of 4-(phenylthio)phthalonitrile metal free dye that can be used in DSSC is analyzed.

2. Experimental

The compound 4-(phenylthio)phthalonitrile was obtained from Aldrich chemicals, U.S.A, and it was used as such to record the FT-IR and FT-Raman spectra. The FT-IR spectrum was recorded by KBr pellet method on a Bruker IFS 66V spectrometer equipped with a Globar source, Ge/KBr beam splitter, and a TGS detector in the range of 4000 to 400 cm^{-1}. The spectral resolution was 2 cm^{-1}. The FT-Raman spectrum of the compound was also recorded in the range 3500 to 50 cm^{-1} using the same instrument with FRA106 Raman module equipped with Nd:YAG laser source operating at 1064 nm line with 200 mW power. A liquid nitrogen cooled–Ge detector was used. The spectrum was recorded at room temperature, with scanning speed of 30 $cm^{-1}min^{-1}$ and the spectral resolution of 2.0 cm^{-1}.

ISSN 2153-2249 (Print) / ISSN 2153-2257 (Online)
DOI:10.5155/eurjchem.2.2.206-213.269

2.1. Computational methods

The computations of the geometries, electronic structures, polarizabilities and hyperpolarizabilities, vibrational frequencies as well as electronic absorption spectrum for dye sensitizer 4-(phenylthio)phthalonitrile were done using Hartree-Fock (HF) and density functional theory (DFT) with Gaussian 03 package [27]. The DFT was treated with hyprid functional Becke's three parameter gradient-corrected exchange potential and the Lee-Yang-Parr (B3LYP) [28-30], and all calculations were performed without any symmetry constraints by using polarized triple-zeta 6-311++G(d,p) basis sets. The PED was calculated using the equation

$$\text{PED} = (F_{ij} L^2_{ik}) / \lambda_k \quad (1)$$

where PED is the combination of the i^{th} symmetry coordinate to the potential energy of the vibration whose frequency is ν_k, F_{ij} are potential constants, L_{ik} are L matrix elements and $\lambda_k = 4\pi^2 C^2 \nu^2_k$ [31]. The vibrational wavenumers were also calculated with above same method and the calculated Raman activities (S_i) were converted to relative Raman intensities (I_i) using the following relationship derived from the intensity theory of Raman scattering [32-34].

$$I_i = \frac{f(\nu_0 - \nu_i)^4 S_i}{\nu_i[1 - \exp(hc\nu_i / kt)]} \quad (2)$$

where ν_0 is the exciting wavenumber in cm^{-1}, ν_i the vibrational wavenumber of the i^{th} normal mode, h, c and k fundamental constants and f is a suitably chosen common normalization factor for all peak intensities. Simulation of calculated FT-IR and FT-Raman spectra have been plotted using pure Lorentzian band shape with a bandwidth (FWHM) of 10 cm^{-1}. The Natural Bonding Orbital (NBO) analysis was performed using restricted Hartree-Fock (RHF) with the 6-311++G(d,p) basis set. The electronic absorption spectrum requires calculation of the allowed excitations and oscillator strengths. These calculations were done using a hybrid method which combines the single-excitation configuration interactions (CIS) with Density Functional Theory (DFT), i.e. CIS-DFT(B3LYP) with the 6-311++G(d,p) basis set in vacuum and acetonitrile solution, and the non-equilibrium version of the polarizable continuum model (PCM) [35,36] was adopted for calculating the solvent effects.

3. Results and discussion

3.1. Geometric structure

The optimized geometry of the 4-(phenylthio) phthalonitrile is shown in Figure 1, and the selected bond lengths, bond angles and dihedral angles are listed in Table 1. The crystal structure of the exact title compound is not available. We can find that most of the optimized bond lengths, bond angles and dihedral angles. The optimized bond lengths of C1-C2 and C3-C4 is 1.4304 and 1.4338 Å, respectively at B3LYP/6-311++G(d,p) and also well matched with HF/6-311++G(d,p).

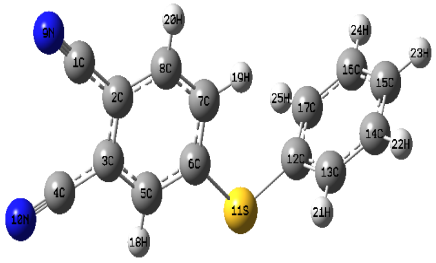

Figure 1. Optimized geometrical structure of dye 4-(phenylthio)phthalonitrile.

Table 1. Bond lengths (Å), bond angles (°) and dihedral angles (°) of the dye 4-(phenylthio)phthalonitrile.

Parameters	HF/6-311++G(d,p)	B3LYP/6-311++G(d,p)
Bond length (Å)		
C1-C2	1.4398	1.4304
C1-N9	1.1298	1.1633
C2-C3	1.3970	1.4166
C2-C8	1.3838	1.4015
C3-C4	1.4426	1.4338
C3-C5	1.3809	1.3971
C4-N10	1.1293	1.1627
C5-C6	1.3919	1.4024
C6-C7	1.3858	1.4017
C6-S11	1.7786	1.7835
C7-C8	1.3833	1.3905
S11-C12	1.7833	1.7952
C12-C13	1.3884	1.4009
C12-C17	1.3884	1.4009
C13-C14	1.3844	1.3952
C14-C15	1.3851	1.3962
C15-C16	1.3851	1.3962
C16-C17	1.3844	1.3953
Bond Angle (°)		
C1-C2-C3	121.6	121.4
C1-C2-C8	119.4	119.8
C3-C2-C8	118.9	118.6
C2-C3-C4	121.1	120.9
C2-C3-C5	120.2	120.0
C4-C3-C5	118.6	119.0
C3-C5-C6	120.5	120.6
C5-C6-C7	119.1	119.2
C5-C6-S11	115.9	116.2
C7-C6-S11	124.8	124.5
C6-C7-C8	120.2	120.2
C2-C8-C7	120.8	121.0
C6-S11-C12	104.3	103.9
S11-C12-C13	119.9	119.9
S11-C12-C17	119.9	119.8
C13-C12-C17	120.0	120.1
C12-C13-C14	119.8	119.7
C13-C14-C15	120.0	120.1
C14-C15-C16	120.1	120.0
C15-C16-C17	120.0	120.1
C12-C17-C16	119.8	119.7
Dihedral Angle (°)		
C1-C2-C3-C5	-180.0	-179.9
C8-C2-C3-C4	-180.0	179.9
C1-C2-C8-C7	-179.9	179.9
C4-C3-C5-C6	180.0	-179.9
C3-C5-C6-S11	-180.0	-179.9
S11-C6-C7-C8	180.0	179.9
C5-C6-S11-C12	-180.0	-179.6
C7-C6-S11-C12	-0.0241	0.4315
C6-S11-C12-C13	91.6	91.2
C6-S11-C12-C17	-91.5	-92.1
S11-C12-C13-C14	177.6	177.1
S11-C12-C13-H21	-2.2	-2.6
C17-C12-C13-C14	0.8524	0.5577
S11-C12-C17-C16	-177.6	-177.1
S11-C12-C17-H25	2.2	2.6
C14-C15-C16-H24	-179.5	-179.6

3.2. Electronic structures and charges

Natural bond orbital (NBO) analysis was performed in order to analyze the charge populations of the dye 4-(phenylthio) phthalonitrile. Charge distributions in C, N and H atoms were observed because of the different electro-negativity, the electrons transferred from C atoms to C, N atoms and C atoms to H. The natural charges of different groups are the sum of every atomic natural charge in the group. These data indicate that the cyanide and amide groups are acceptors, while the acetic groups are donors, and the charges were transferred through chemical bonds. The frontier molecular orbitals (MO) energies and corresponding density of state of the dye 4-(phenylthio)phthalonitrile is shown in Figure 2. The HOMO-LUMO gap of the dye 4-(phenylthio)phthalonitrile in vacuum is 3.87 eV.

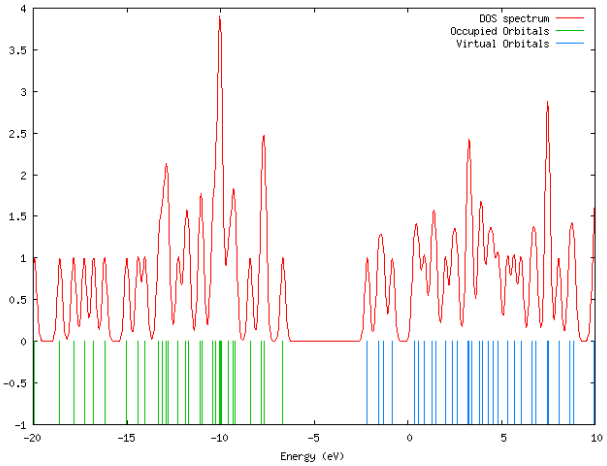

Figure 2. The frontier molecular orbital energies and corresponding density of state (DOS) spectrum of the dye 4-(phenylthio)phthalonitrile.

While the calculated HOMO and LUMO energies of the bare $Ti_{38}O_{76}$ cluster as a model for nanocrystalline are -6.55 and -2.77 eV, respectively, resulting in a HOMO-UMO gap of 3.78 eV, the lowest transition is reduced to 3.20 eV according to TD-DFT, and this value is slightly smaller than typical band gap of TiO_2 nanoparticles with nm size [37]. Furthermore, the HOMO, LUMO and HOMO-LUMO gap of $(TiO_2)_{60}$ cluster is -7.52, -2.97, and 4.55 eV (B3LYP/VDZ), respectively [38]. Taking into account of the cluster size effects and the calculated HOMO, LUMO, HOMO-LUMO gap of the dye 4-(phenylthio) phthalonitrile, $Ti_{38}O_{76}$ and $(TiO_2)_{60}$ clusters, we can find that the HOMO energies of these dyes fall within the TiO_2 gap.

The above data also reveal the interfacial electron transfer between semiconductor TiO_2 electrode and the dye sensitizer 4-(phenylthio)phthalonitrile is electron injection processes from excited dye to the semiconductor conduction band. This is a kind of typical interfacial electron transfer reaction [39].

3.3. IR and Raman frequencies

Figure 3 and 4 shows the observed and calculated IR and Raman spectra of 4-(phenylthio)phthalonitrile respectively. Comparison of the observed (FT-IR and FT-Raman) and calculated vibrational frequencies of 4-(phenylthio) phthalonitrile is shown in Table 2. Comparison of the frequencies calculated by HF and B3LYP with experimental values reveals the overestimation of the calculated vibrational modes due to neglect of anharmonicity. A corrective vibrational scaling factor of 0.9613 [40,41] to B3LYP calculated frequencies and scaling factor of 0.8982 [40,41] to HF calculated frequencies were applied to account for anharmonicity. Inclusion of electron correlation in density functional theory to a certain extent makes the frequency values smaller in comparison with experimental values. Any way notwithstanding the level of calculations it is customary to scale down the calculated harmonic frequencies in order to improve the agreement with the experiment.

The 4-(phenylthio)phthalonitrile molecule give rise to three C-C inplane bending vibrations at 2, 27 and 366 cm^{-1}, one C-N inplane bending vibration at 264 cm^{-1}, three C-C out-of-plane bending vibrations at 49, 136 and 212 cm^{-1}, two C-N out-of-plane bending vibrations at 136 and 212 cm^{-1}, twenty four C-C-C ring deformations at 81, 136, 232, 264, 284, 366, 386, 434, 450, 495, 532, 618, 628, 648, 713, 733, 878, 1014, 1047, 1102, 1108, 1150, 1218 and 1303 cm^{-1}, seven C-C torsions at 416, 434, 450, 495, 532, 861 and 982 cm^{-1}, six C-C-N inplane bending vibrations at 113, 450, 495, 532, 618 and 648 cm^{-1}, three C-C ring breathing at 547, 612 and 739 cm^{-1}, two C-C-C out-of-plane bending vibrations at 705 and 713 cm^{-1}, five C-C stretching vibrations at 733, 769, 878, 941 and 1218 cm^{-1}, twenty three C-H wagging at 769, 844, 941, 978, 1010, 1093, 1102, 1108, 1150, 1189, 1205, 1218, 1245, 1303, 1325, 1427, 1480, 1518, 1521, 1586, 1631, 1632 and 1639 cm^{-1}, one C-H stretching vibration at 907 cm^{-1}, four C-C symmetrical stretching vibrations at 1245, 1427, 1480 and 1521 cm^{-1}, six C-C asymmetrical stretching vibrations at 1329, 1352, 1586, 1631, 1632 and 1639 cm^{-1}, one C≡N symmetrical stretching vibration at 2348 cm^{-1}, one C≡N asymmetrical stretching vibration at 2355 cm^{-1}, five C-H asymmetrical stretching vibrations at 3187, 3196, 3205, 3210 and 3214 cm^{-1} and three C-H symmetrical stretching vibrations at 3213, 3217 and 3230 cm^{-1} were assigned to B3LYP/6-311++G(d,p) scaling method.

The strongest IR absorption for 4-(phenylthio) phthalonitrile corresponds to the vibrational mode 58 near about 1632 cm^{-1}, which is corresponding to stretching mode of C=C bonds. The next stronger IR absorption is attributed to vibrational mode 60 near about 2348 cm^{-1}, corresponding to the stretching mode of C-N triple bond. In the Raman spectrum, however, the strongest activity mode is the vibrational mode 60 near about 2348 cm^{-1}, which is corresponding to stretching mode of C-N triple bond. The same vibrations computed by HF/6-311++G(d,p) and also shows good agreement with experimental data.

3.4. Polarizability and hyperpolarizability

Polarizabilities and hyperpolarizabilities characterize the response of a system in an applied electric field [42]. They determine not only the strength of molecular interactions (long-range intermolecular induction, dispersion forces, etc.) as well as the cross sections of different scattering and collision processes, but also the nonlinear optical properties (NLO) of the system [43,44]. It has been found that the dye sensitizer hemicyanide system, which has high NLO property, usually possesses high photoelectric conversion performance [45].

In order to investigate the relationships among photocurrent generation, molecular structures and NLO, the polarizabilities and hyperpolarizabilities of 4-(phenylthio) phthalonitrile was calculated. Here, the polarizability and the first hyperpolarizabilities are computed using B3LYP/6-311++G(d,p) method. The definitions [43,44] for the isotropic polarizability is

$$\alpha = \frac{1}{3}\left(\alpha_{XX} + \alpha_{YY} + \alpha_{ZZ}\right) \quad (3)$$

Table 2. Comparison of the observed (FT-IR and FT-Raman) and calculated vibrational frequencies of 4-(phenylthio)phthalonitrile*.

Vib. mode no	Species	Experimental Wavenumber (cm^{-1})		IR Intensity	Raman intensity	Scaled Wavenumber (cm^{-1})		Scaled IR Intensity (KM/ Mole)	Raman active (A^4/ AMU)	Assignments PED (%)
		FT-IR	FT-Raman			HF 6-311++G(d,p)	B3LYP 6-311++G(d,p)			
1	A’	-	-	-	-	6	2	0.5	6.0	β C-C (96)
2	A’	-	-	-	-	44	27	0.1	12.4	β C-C (95)
3	A’’	-	-	-	-	56	49	0.5	8.8	γ C-C (92)
4	A’	-	-	-	-	92	81	3.7	0.6	δ C-C (98)
5	A’	-	110 vw	-	5.9	128	113	1.4	5.5	β C-C-N (67)
6	A’	-	-	-	-	148	136	2.7	0.8	δ C-C (74)
7	A’’	-	-	-	-	151	136	4.4	1.9	γ C-N(53) + γ C-C (41)
8	A’’	-	215 vw	-	3.6	234	212	0.3	3.8	γ C-N (69) + γ C-C (27)
9	A’	-	-	-	-	254	232	2.9	0.1	δ C-C (99)
10	A’	-	-	-	-	290	264	3.9	4.9	β C-N (76) + δ C-C (19)
11	A’’	-	-	-	-	307	284	0.1	0.4	δ C-C (91)
12	A’	-	-	-	-	393	366	0.4	2.6	δ C-C (61) + β C-C (22)
13	A’’	-	-	-	-	424	386	0.6	2.4	δ C-C (93)
14	A’’	-	-	-	-	455	416	0.1	0.1	τ C-C (98)
15	A’	420 vw	441 vw	3.1	2.4	471	434	3.3	1.9	δ C-C (67) + τ C-C (18)
16	A’’	-	-	-	-	478	434	1.8	1.7	δ C-C (54) + τ C-C (35)
17	A’	-	-	-	-	484	450	0.9	4.5	β C-C-N (34) + δ C-C (26) + τ C-C (21)
18	A’	479 w	488 vw	6.1	6.5	550	495	6.4	6.9	β C-C-N (49) +δ C-C (30) + τ C-C (12)
19	A’	519 w	-	6.2	-	580	532	6.3	1.8	β C-C-N (43) + δ C-C (25) + τ C-C (18)
20	A’	526 w	540 vw	11.5	6.2	609	547	11.9	6.9	Rb C-C (87)
21	A’	-	-	-	-	669	612	0.1	1.2	Rb C-C (68)
22	A’’	603 vw	609 vw	3.2	5.1	669	618	3.6	5.3	β C-C-N (43) + δ C- C(34)
23	A’	-	614 vw	-	5.7	673	628	0.1	5.4	δ C-C (98)
24	A’’	-	-	-	-	711	648	1.6	0.7	β C-C-N (67) + δ C-C(22)
25	A’’	698 w	-	13.2	-	762	705	13.8	0.6	γ C-C-C (89)
26	A’	705 w	-	11.3	-	768	713	11.4	2.4	δ C-C (62) + γ C-C-C (23)
27	A’	722 vw	720 w	5.0	19.1	781	733	5.2	17.3	υ C-C (52) + δ C-C (34)
28	A’	-	-	-	-	816	739	0.1	0.4	Rb C-C (96)
29	A’’	744	-	25.9	-	847	769	26.8	3.9	γ C-C (72) + ω C-H (19)
30	A’	832 w	-	19.8	-	939	844	20.3	0.6	ω C-H(79)
31	A’	-	855 vw	-	6.2	944	861	0.4	5.3	τ C-C (83)
32	A’	865 m	869 vw	25.3	10.4	955	878	25.9	9.4	υ C-C (65) + δ C-C (29)
33	A’	-	-	-	-	1013	907	7.1	3.2	υ C-H (85)
34	A’’	-	-	-	-	1053	941	1.5	1.2	υ C-C (48) + ωC-H (27)
35	A’’	-	-	-	-	1083	978	0.8	1.1	ω C-H (91)
36	A’	-	-	-	-	1100	982	0.1	0.2	τ C-C (94)
37	A’	-	-	-	-	1108	1010	0.1	0.1	ω C-H (94)
38	A’	1008 w	1007 w	9.1	34.6	1113	1014	9.6	31.9	δ C-C (82)
39	A’	1032 w	1033 w	5.6	31.4	1126	1047	5.9	26.3	δ C-C (88)
40	A’’	1057 m	1059 m	20.9	52.5	1164	1093	21.5	48.5	ω C-H (76)
41	A’’	-	-	-	-	1168	1102	2.8	0.5	δ C-C (66) + ω C-H (25)
42	A’	-	1102 m	-	54.1	1196	1108	0.7	49.5	δ C-C (57) + ω C-H (34)
43	A’	1141 w	-	19.6	-	1196	1150	20.1	1.8	δ C-C (55) + ω C-H (29)
44	A’’	-	1178 vw	-	6.7	1209	1189	0.1	5.9	ω C-H (92)
45	A’	1196 vw	1193 vw	3.6	8.0	1253	1205	3.8	7.1	ω C-H (99)
46	A’	1205 v	1205 vw	9.6	12.8	1287	1218	10.0	13.4	δ C-C (46) + υ C-C (26) + ω C-H (17)
47	A’	1223 v	1240 s	8.9	141.3	1306	1245	9.2	137.7	υsym C-C (72)+ ωC-H (15)
48	A’’	-	1295 vw	-	12.2	1315	1303	1.7	10.6	δ C-C(46) + ω C-H (30)
49	A’	-	-	-	-	1326	1325	0.1	0.2	ω C-H (90)
50	A’	-	-	-	-	1408	1329	6.2	4.3	υasy C-C (94)
51	A’	1311 vw	-	2.6	-	1448	1352	3.0	3.1	υasy C-C (95)
52	A’	1408 w	1415 vw	6.0	4.5	1531	1427	6.2	5.1	υsym C-C (86) + ω C-H (10)
53	A’	1444 w	-	8.2	-	1586	1480	8.7	2.3	υsym C-C (55) + ω CH (41)
54	A’	1469 m	-	23.6	-	1635	1518	24.4	4.9	ω C-H (92)
55	A’’	1503 m	1518 w	28.1	41.8	1650	1521	28.4	39.7	υsym C-C (51) + ω C-H (33)
56	A’	1566 m	1572 m	22.9	74.5	1734	1586	23.3	72.5	υasy C-C (54) + ω C-H (44)
57	A’	-	-	-	-	1759	1631	1.0	7.9	υasy C-C (62) + ω C-H (25)
58	A’	1618 vs	1618 vs	109.8	276.2	1771	1632	112.2	266.5	υ_{asy} C-C (39) + ω C-H (49)
59	A’	1625 w	1617 m	10.6	82.7	1777	1639	10.8	79.8	υ_{asy} C-C (57) + ω C-H (41)
60	A’’	2331 s	2329 vs	34.9	865.3	2593	2348	35.6	842.6	υ_{sym} C≡N (96)
61	A’	2345 w	2343 vs	6.7	390.6	2599	2355	6.9	354.4	υ_{asy} C≡N (96)
62	A’	-	3174 w	-	41.8	3326	3187	0.1	36.9	υ_{asy} C-H (98)
63	A’	3175 vw	3181 s	4.8	142.9	3337	3196	5.1	133.4	υ_{asy} C-H (87)
64	A’’	3189 w	3198 s	12.4	119.0	3347	3205	12.6	105.5	υ_{asy} C-H (81)
65	A’	-	3204 w	-	49.3	3355	3210	0.1	42.5	υ_{asy} C-H (76)
66	A’	3208 w	3210 vw	9.6	4.6	3356	3213	9.9	6.5	υ_{sym} C-H (91)
67	A’	-	3212 m	-	81.0	3359	3214	0.7	73.7	υ_{asy} C-H (95)
68	A’’	3211 w	3216 vs	7.5	289.5	3360	3217	7.8	309.9	υ_{sym} C-H (92)
69	A’	-	3226 s	-	102.7	3382	3230	0.7	97.3	υ_{sym} C-H (94)

* w-weak; vw-very weak; s-strong; vs-very strong; m-medium; υ - stretching; υ_{sym}-symmetric stretching; υ_{asy}-asymmetric stretching; β-in plane bending; γ- out-of-plane bending; ω-wagging; τ- torsion ; δ- Ring deformation; R_b- Ring breathing.

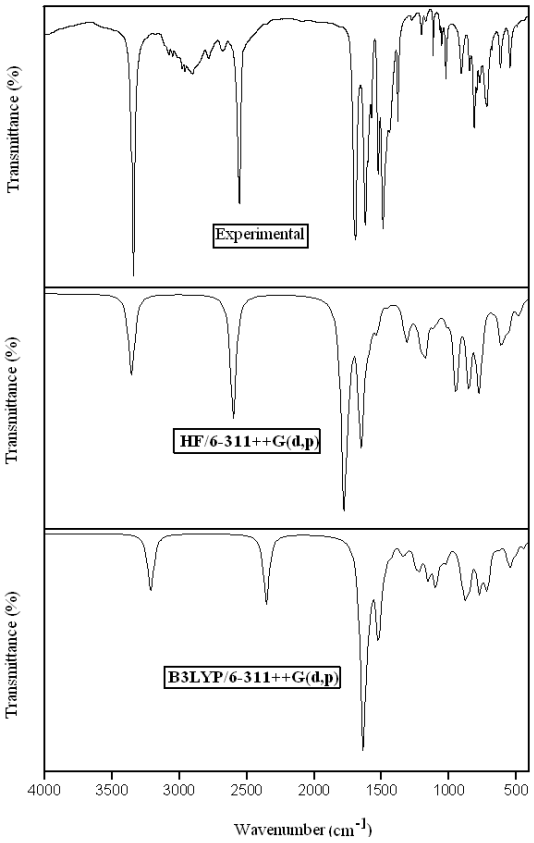

Figure 3. Observed and calculated FT-IR spectra of 4-(phenylthio)phthalonitrile.

The polarizability anisotropy invariant is

$$\Delta\alpha = \left[\frac{(\alpha_{XX}-\alpha_{YY})^2+(\alpha_{YY}-\alpha_{ZZ})^2+(\alpha_{ZZ}-\alpha_{XX})^2}{2}\right]^{\frac{1}{2}} \quad (4)$$

and the average hyperpolarizability is

$$\beta_{\parallel} = \frac{1}{5}\sum_i(\beta_{iiZ}+\beta_{iZi}+\beta_{Zii}) \quad (5)$$

Where, α_{XX}, α_{YY}, and α_{ZZ} are tensor components of polarizability; β_{iiZ}, β_{iZi}, and β_{Zii} (i from X to Z) are tensor components of hyperpolarizability.

Tables 3 and 4 list the values of the polarizabilities and hyperpolarizabilities of the dye 4-(phenylthio)phthalonitrile. In addition to the individual tensor components of the polarizabilties and the first hyperpolarizabilities, the isotropic polarizability, polarizability anisotropy invariant and hyperpolarizability are also calculated. The calculated isotropic polarizability of 4-(phenylthio)phthalonitrile is 113.75 a.u. However, the calculated isotropic polarizability of JK16, JK17, dye 1, dye 2, D5, DST and DSS is 759.9, 1015.5, 694.7, 785.7, 510.6, 611.2 and 802.9 a.u., respectively [46,47]. The above data indicate that the donor-conjugate π bridge-acceptor (D-π-A) chain-like dyes have stronger response for external electric field. Whereas, for dye sensitizers D5, DST, DSS, JK16, JK17, dye 1 and dye 2, on the basis of the published photo-to-current conversion efficiencies, the similarity and the difference of geometries, and the calculated isotropic polarizabilities, it is found that the longer the length of the conjugate bridge in similar dyes, the larger the polarizability of the dye molecule, and the lower the photo-to-current conversion efficiency. This may be due to the fact that the longer conjugate π bridge enlarged the delocalization of electrons, thus it enhanced the response of the external field, but the enlarged delocalization may be not favorable to generate charge separated state effectively. So it induces the lower photo-to-current conversion efficiency.

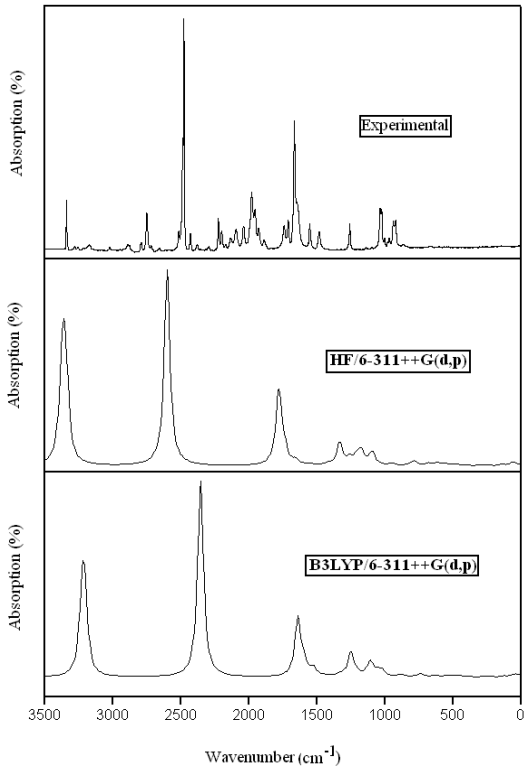

Figure 4. Observed and calculated FT-Raman spectra of 4-(phenylthio)phthalonitrile.

3.5. Electronic absorption spectra and sensitized mechanism

The calculated electronic absorption spectra of 4-(phenylthio)phthalonitrile in solvent were performed using CIS-DFT(B3LYP)/6-311++G(d,p) calculations, and compared with experimental results are shown in Figure 5. It is observed that the absorption in the visible region is much weaker than that in the UV region for 4-(phenylthio)phthalonitrile. The results of CIS-DFT have an appreciable red-shift in experimental results, and the degree of red-shift in scaled spectrum is more significant than that in observed spectrum. The discrepancy between observed and scaled effects in CIS-DFT calculations may result from two aspects. The first aspect is smaller gap of materials which induces smaller excited energies. The other is solvent effects. Experimental measurements of electronic absorptions are usually performed in solution. Solvent, especially polar solvent, could affect the geometry and electronic structure as well as the properties of molecules through the long-range interaction between solute molecule and solvent molecule. For these reasons it is more difficult to make that the CIS-DFT calculation is consistent with quantitatively. Though the discrepancy exists, the CIS-DFT calculations are capable of describing the spectral features of 4-(phenylthio)phthalonitrile because of the agreement of line shape and relative strength as compared with the observed and scaled spectrum.

Table 3. Polarizability (α) of the dye 4-(phenylthio)phthalonitrile (in a.u.).

α_{xx}	α_{xy}	α_{yy}	α_{xz}	α_{yz}	α_{zz}	α	Δα
-134.36	9.18	-108.54	0.89	0.095	-98.36	113.75	32.14

Table 4. Hyperpolarizability (β) of the dye 4-(phenylthio)phthalonitrile (in a.u.).

β_{xxx}	β_{xxy}	β_{xyy}	β_{yyy}	β_{xxz}	β_{xyz}	β_{yyz}	β_{xzz}	β_{yzz}	β_{zzz}	β_{ii}
334.53	14.20	50.90	-6.29	6.06	0.38	0.83	21.19	1.86	2.18	5.45

Table 5. Computed excitation energies, electronic transition configurations and oscillator strengths (f) for the optical transitions with f > 0.01 of the absorption bands in visible and near-UV region for the dye 4-(phenylthio)phthalonitrile in acetonitrile.

State	Configurations composition (corresponding transition orbitals)	Excitation energy (eV/nm)	Oscillator strength (f)
1	0.66887 (61 → 62)	3.2499/ 381.51	0.2253
2	0.13975 (58 → 62) 0.66811 (61 → 63)	3.9511/ 313.80	0.2232
3	0.70023 (60 → 62)	4.2507 /291.68	0.0052
4	0.46761 (58 → 62) 0.10808 (58 → 63) -0.40134 (59 → 62) 0.26453 (59 → 63)	4.6874/264.51	0.1085
5	0.67787 (61 → 65)	4.8433/255.99	0.0021
6	0.33154 (58 → 62) 0.51383 (59 → 62) 0.21760 (59 → 63)	4.8645/ 254.88	0.1672
7	0.41959 (60→ 63) 0.20742 (60 → 66) 0.51766 (61 → 64)	4.9645 / 249.74	0.0034
8	0.56264 (60 → 63) -0.17895 (60 → 66) -0.36540 (61 → 64)	5.1390 /241.26	0.0493
9	0.15895 (57 → 62) -0.10318 (58 → 62) 0.24243 (59 → 63) -0.10036 (61 → 64) 0.57832 (61 → 66)	5.3342 / 232.43	0.4372
10	0.14448 (54→ 62) 0.68528 (56 → 62)	5.5101 / 225.01	0.0003
11	0.60981 (57 → 62) -0.13514 (58 → 62) 0.11602 (59 → 63) -0.21191 (61 → 66)	5.5796 / 222.21	0.0084
12	0.35241 (53 → 62) 0.53317 (55 → 62) 0.23153 (61 → 67)	5.7441 / 215.85	0.0000
13	-0.21734 (57→ 62) -0.19610 (58 → 62) -0.16645 (58 → 63) 0.51223 (59→ 63) 0.11368 (60→ 64) -0.14277 (61→ 66)	5.7481 / 215.70	0.3597
14	-0.12424 (53→ 62) -0.21906 (55 → 62) 0.11640 (59 → 67) 0.61745 (61 → 67)	5.8203 / 213.02	0.0002
15	-0.15604 (52 → 62) 0.64503 (54 → 62) -0.10637 (54 → 63) -0.13673 (56 → 62)	5.8896 / 210.51	0.0001
16	0.12330 (51→ 62) -0.10698 (57 → 62) 0.59711 (58 → 63)	5.9477 / 208.46	0.2996
17	0.68553 (60 → 65) -0.11840 (60 → 67)	5.9619 / 207.96	0.0000
18	0.14075 (59 → 65) 0.10820 (61 → 67) 0.58798 (61 → 68) -0.31410 (61 → 69)	6.0484 / 204.99	0.0002
19	-0.14062 (57→ 64) 0.12309 (58 → 64) -0.40807 (59 → 64) -0.10260 (59→ 66) -0.10668 (60→ 64) 0.46306 (60→ 66) -0.19168 (61→ 64)	6.1484 / 201.65	0.0442
20	0.39529 (56 → 63) 0.27616 (59 → 65) -0.28579 (61 → 68) -0.38909 (61 → 69)	6.2619 / 198.00	0.0000

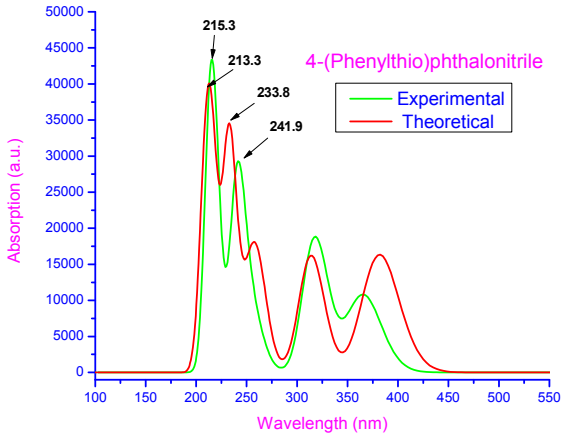

Figure 5. Electronic absorption spectra of the dye 4-(phenylthio)phthalonitrile.

The HOMO-LUMO gap of 4-(phenylthio)phthalonitrile in acetonitrile at CIS-DFT/6-311++G(d,p) theory level is smaller than that in experimental. This fact indicates that the solvent effects stabilize the frontier orbitals of 4-(phenylthio) phthalonitrile. So it induces the smaller intensities and red-shift of the absorption as compared with that in experimental. In order to obtain the microscopic information about the electronic transitions, the corresponding MO properties are checked. The absorption in visible and near-UV regions is the most important region for photo-to-current conversion, so only the twenty lowest singlet/singlet transitions of the absorption band in visible and near-UV region for 4-(phenylthio) phthalonitrile is listed in Table 5. The data of Table 5 and Figure 6 are based on the CIS-DFT/6-311++G(d,p) results with solvent effects involved.

This indicates that the transitions are photoinduced charge transfer processes, thus the excitations generate charge separated states, which should favour the electron injection from the excited dye to semiconductor surface.

The solar energy to electricity conversion efficiency (η) under AM 1.5 white-light irradiation can be obtained from the following formula:

$$\eta(\%) = \frac{J_{SC}[mAcm^{-2}]V_{OC}[V]ff}{I_0[mWcm^{-2}]} \times 100 \quad (6)$$

where I_0 is the photon flux, J_{sc} is the short-circuit photocurrent density, and V_{oc} is the open-circuit photovoltage, and ff represents the fill factor [48]. At present, the J_{sc}, the V_{oc}, and the ff are only obtained by experiment, the relationship among these quantities and the electronic structure of dye is still unknown. The analytical relationship between V_{oc} and E_{LUMO} may exist. According to the sensitized mechanism (electron injected from the excited dyes to the semiconductor conduction band) and single electron and single state approximation, there is an energy relationship:

$$eV_{oc} = E_{LUMO} - E_{CB} \quad (7)$$

where, E_{CB} is the energy of the semiconductor's conduction band edge. So the V_{oc} may be obtained applying the following formula:

$$V_{oc} = \frac{(E_{LUMO} - E_{CB})}{e} \quad (8)$$

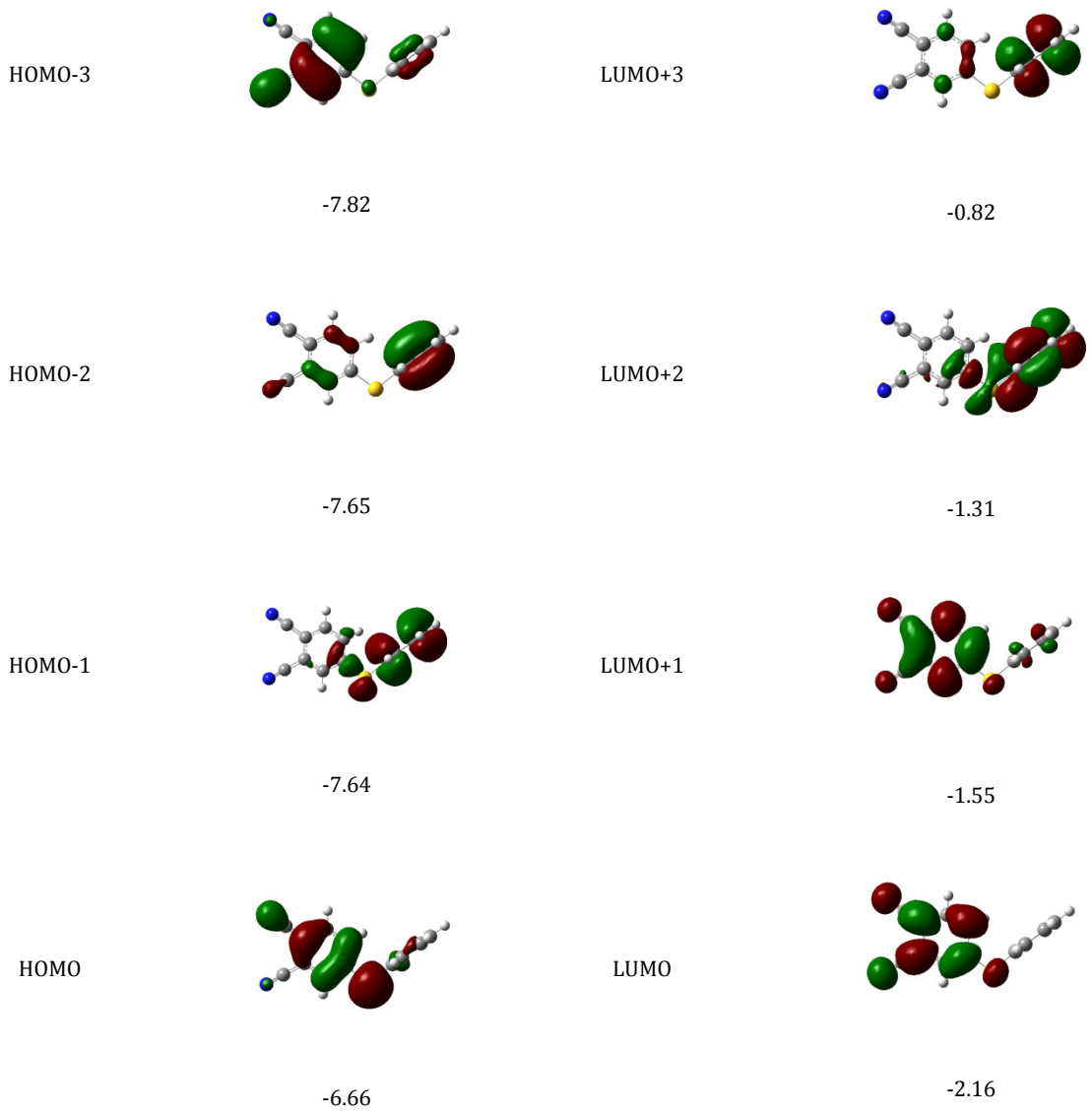

Figure 6. Isodensity plots (isodensity contour = 0.02 a.u.) of the frontier orbitals of the dye 4-(phenylthio)phthalonitrile and corresponding orbital energies (in eV).

It induces that the higher the E_{LUMO}, the larger the V_{oc}. The results of organic dye sensitizer JK16 and JK17 [46], D-ST and D-SS also proved the tendency [49] (JK16: E_{LUMO} = -2.73 eV, V_{oc} = 0.74 V; JK17: E_{LUMO} = -2.87 eV, V_{oc} =0.67 V; D-SS: E_{LUMO} = -2.91 eV, V_{oc} = 0.70 V; D-ST: E_{LUMO} = -2.83 eV, V_{oc} = 0.73 V). Certainly, this formula expects further test by experiment and theoretical calculation.

The J_{sc} is determined by two processes, one is the rate of electron injection from the excited dyes to the conduction band of semiconductor, and the other is the rate of redox between the excited dyes and electrolyte. Electrolyte effect on the redox processes is very complex, and it is not taken into account in the present calculations. This indicates that most of excited states of 4-(phenylthio)phthalonitrile have larger absorption coefficient, and then with shorter lifetime for the excited states, so it results in the higher electron injection rate which leads to the larger J_{sc} of 4-(phenylthio) phthalonitrile. On the basis of above analysis, it is clear that the 4-(phenylthio)phthalonitrile has better performance in DSSC.

4. Conclusions

The geometries, electronic structures, polarizabilities, and hyperpolarizabilities of dye 4-(phenylthio)phthalonitrile were studied by using HF and DFT with hybrid functional B3LYP, and the UV-Vis spectra were investigated by using CIS-DFT methods. The NBO results suggested that 4-(phenylthio) phthalonitrile is a (D-π-A) system. The calculated isotropic polarizability of 4-(phenylthio)phthalonitrile is 113.75 a.u. The calculated polarizability anisotropy invariant of 4-(phenylthio) phthalonitrile is 32.14 a.u. The hyperpolarizability of 4-(phenylthio)phthalonitrile is 5.4526 (in a.u). The strongest IR absorption for 4-(phenylthio)phthalonitrile corresponds to the vibrational mode 58 near about 1632 cm^{-1}, which is corresponding to stretching mode of C=C bonds. The next stronger IR absorption is attributed to vibrational mode 60 near about 2348 cm^{-1}, corresponding to the stretching mode of C-N triple bond. In the Raman spectrum, however, the strongest activity mode is the vibrational mode 60 near about 2348 cm^{-1}, which is corresponding to stretching mode of C-N triple bond.

The electronic absorption spectral features in visible and near-UV region were assigned based on the qualitative agreement to CIS-DFT calculations. The absorptions are all ascribed to $n \rightarrow \pi^*$ transition. The three excited states with the lowest excited energies of 4-(phenylthio)phthalonitrile is photoinduced electron transfer processes that contributes sensitization of photo-to-current conversion processes. The interfacial electron transfer between semiconductor TiO_2 electrode and dye sensitizer 4-(phenylthio)phthalonitrile is electron injection process from excited dye as donor to the semiconductor conduction band. Based on the analysis of geometries, electronic structures, and spectrum properties of 4-(phenylthio)phthalonitrile, the role of phenylthio group in phthalonitrile is as follows: it enlarged the distance between electron donor group and semiconductor surface, and decreased the timescale of the electron injection rate, resulted in giving lower conversion efficiency. This indicates that the choice of the appropriate conjugate bridge in dye sensitizer is very important to improve the performance of DSSC.

Acknowledgements

This work was partly financially supported by University Grants Commission, Govt. of India, New Delhi, within the Major Research Project scheme under the approval-cum-sanction Nos. F.No.34-5\2008(SR) and 34-1/TN/08.

References

[1]. O'Regan, B.; Gratzel, M. *Nature* **1991,** *353*, 737-739.
[2]. Gratzel, M. *Nature* **2001**, *414*, 338-344.
[3]. Park, N. G.; Kim, K. *Phys. Status Solid A* **2008**, *205*, 1895-1904.
[4]. Chiba, Y.; Islam, A.; Watanabe, Y.; Komiya, R.; Koide, N.; Han, L. *Jpn. J. Appl. Phys*. **2006**, *45*, L638-L640.
[5]. Hara, K.; Kurashige, M.; Dan-Oh, Y.; Kasada, C.; Shinpo, A.; Suga, S.; Sayama, K.; Arakawa, H. *New J. Chem*. **2003**, *27*, 783-785.
[6]. Kitamura, T.; Ikeda, M.; Shigaki, K.; Inoue, T.; Anderson, N. A.; Ai, X.; Lian, T.; Yanagida, S. *Chem. Mater*. **2004**, *16*, 1806-1812.
[7]. Horiuchi, T.; Miura, H.; Sumioka, K.; Uchida, S. *J. Am. Chem. Soc*. **2004**, *126*, 12218-12219.
[8]. Campbell, W. M.; Burrell, A. K.; Officer, D. L.; Jolley, K. W. *Coord. Chem. Rev*. **2004**, *248,* 1363-1379.
[9]. Thomas, K. R. J.; Lin, J. T.; Hsu, Y. C.; Ho, K. C. *Chem. Commun*. **2005**, *32*, 4098-4100.
[10]. Hagberg, D. P.; Edvinsson, T.; Marinado, T.; Boschloo, G.; Hagfeldt, A.; Sun, L. *Chem. Commun*. **2006**, *21*, 2245-2247.
[11]. Li, S. L.; Jiang, K. J.; Shao, K. F.; Yang, L. M. *Chem. Commun*. **2006**, *26*, 2792-2794.
[12]. Koumura, N.; Wang, Z. S.; Mori, S.; Miyashita, M.; Suzuki, E.; Hara, K. *J. Am. Chem. Soc*. **2006**, *128*, 14256-14257.
[13]. Kim, S.; Lee, J. W.; Kang, S. O.; Ko, J.; Yum, J. H.; Fantacci, S.; De Angellis, F.; Di Censo, D.; Nazeeruddin, M. K.; Gratzel, M. J. *J. Am. Chem. Soc*. **2006**, *128*, 16701-16707.
[14]. Wang, Z. S.; Cui, Y.; Hara, K.; Dan-oh, Y.; Kasada, C.; Shinpo, A. *Adv. Mater*. **2007**, *19*, 1138-1141.
[15]. Edvinsson, T.; Li, C.; Pschirer, N.; Schoneboom, J.; Eickemeyer, F.; Sens, R.; Boschloo, G.; Herrmann, A.; Mullen, K.; Hagfeldt, A. *J. Phys. Chem. C* **2007**, *111*, 15137-15140.
[16]. Wang, M.; Xu, M.; Shi, D.; Li, R.; Gao, F.; Zhang, G.; Yi, Z.; Humphry-Baker, R.; Wang, P.; Zakeeruddin, S. M.; Gratzel, M. *Adv. Mater*. **2008**, *20*, 4460-4463.
[17]. Shi, D.; Pootrakuchote, N.; Yi, Z.; Xu, M.; Zakeeruddin, S. M.; Gratzel, M.; Wang, P. J. *J. Phys. Chem. C* **2008**, *112*, 17478-17484.
[18]. Zhou, G.; Pschirer, N.; Schoneboom, J. C.; Eickemeyer, F.; Baumgarten, M.; Mullen, K. *Chem. Mater*. **2008**, *20*, 1808-1815.
[19]. Lin, J. T.; Chen, P. C.; Yen, Y. S.; Hsu, Y. C.; Chou, H. H.; Yeh, M. C. P. *Org. Lett*. **2009**, *11*, 97-100.
[20]. Zhang, G.; Bai, Y.; Li, R.; Shi, D.; Wenger, S.; Zakeeruddin, S. M.; Gratzel, M.; Wang, P. *Energy Environs. Sci*. **2009**, *2*, 92-95.
[21]. Xu, M.; Wenger, S.; Bara, H.; Shi, D.; Li, R.; Zhou, Y.; Zakeeruddin, S. M.; Gratzel, M.; Wang, P. *J. Phys. Chem. C* **2009**, *113*, 2966-2973.
[22]. Zhang, X. H.; Li, C.; Wang, W. B.; Cheng, X. X.; Wang, X. S.; Zhang, B. W. *J. Mater. Chem*. **2007**, *17*, 642-649.
[23]. Liang, M.; Xu, W.; Cai, F.; Chen, P.; Peng, B.; Chen, J.; Li, Z. *J. Phys. Chem. C* **2007**, *111*, 4465-4472.
[24]. Xu, W.; Peng, B.; Chen, J.; Liang, M.; Cai, F. *J. Phys. Chem. C* **2008**, *112*, 874-880.
[25]. Ito, S.; Miura, H.; Uchida, S.; Takata, M.; Sumioka, K.; Liska, P.; Comte, P.; Pechy, P.; Gratzel, M. *Chem. Commun*. **2008**, *41*, 5194-5196.
[26]. Filippo De Angellis; Antonio Tilocca; Annabella Selloni. *J. Am. Chem. Soc*. **2004**, *126*, 15024-15025.
[27]. Frisch, M. J.; Trucks, G. W.; Schlegel, H. B.; Scuseria, G. E.; Robb, M. A.;Cheeseman, J. R.; Montgomery Jr., J. A.; Vreven, T.; Kudin, K. N.;Burant, J. C.; Millam, J. M.; Iyengar, S. S.; Tomasi, J.; Barone, V.; Mennucci, B.; Cossi, M.; Scalmani, G.; Rega, N.; Petersson, G. A.; Nakatsuji, H.; Hada, M.; Ehara, M.; Toyota, K.; Fukuda, R.; Hasegawa, J.; Ishida, M.; Nakajima, T.; Honda, Y.; Kitao, O.; Nakai, H.; Klene, M.; Li, X.; Knox, J. E.; Hratchian, H. P.; Cross, J. B.; Adamo, C.; Jaramillo, J.; Gomperts, R.; Stratmann, R. E.; Yazyev, O.; Austin, A. J.; Cammi, R.; Pomelli, C.; Ochterski, J. W.; Ayala, P. Y.; Morokuma, K.; Voth, G. A.; Salvador, P.; Dannenberg, J. J.; Zakrzewski, V. G.; Dapprich, S.; Daniels, A. D.; Strain, M. C.; Farkas, O.; Malick, D. K.; Rabuck, A. D.; Raghavachari, K.; Foresman, J.B.; Ortiz, J. V.; Cui, Q.; Baboul, A. G.; Clifford, S.; Cioslowski, J.; Stefanov, B. B.; Liu, G.; Liashenko, A.; Piskorz, P.; Komaromi, I.; Martin, R. L.; Fox, D. J.; Keith, T.; Al-Laham, M. A.; Peng, C. Y.; Nanayakkara, A.; Challacombe, M.; Gill, P. M. W.; Johnson, B.; Chen, W.; Wong, M. W.; Gonzalez, C.; Pople, J. A. Gaussian 03, Gaussian, Inc., Pittsburgh, *PA*, 2003.
[28]. Becke, A. D. *J. Chem. Phys*. **1993**, *98*, 5648-5652.
[29]. Miehlich, B.; Savin, A.; Stoll, H.; Preuss, H. *Chem. Phys. Lett.* **1989**, *157*, 200-206.
[30]. Lee, C.; Yang, W.; Parr, R. G. *Phys. Rev. B* **1988**, *37*, 785-789.
[31]. Mohan, S.; Sonamuthu, S.; Sujin P, Jose. *J. Phy. Sci.* **2006**, *17*, 27-35.
[32]. Polavarapu, P. L. *J. Phy. Chem.,* **1990**, *94*, 8106-8112.
[33]. Keresztery, G.; Holly, S.; Varga, J.; Besenyei, G.; Wang, A.Y.; Durig, J. R. *Spectrochim. Acta* **1993**, *49A*, 2007-2017.
[34]. Keresztery, G. Raman Spectroscopy: *Theory in Handbook of vibrational Spectroscopy*, vol. 1 [Eds: Chalmers, J. M.; Griffiths], John Wiley and sons: 2002, pp. 71.
[35]. Barone, V.; Cossi, M. *J. Phys. Chem. A* **1998**, *102*, 1995-2001.
[36]. Cossi, M.; Rega, N.; Scalmani, G.; Barone, V. *J. Comput. Chem*. **2003**, *24*, 669-681.
[37]. Nazeeruddin, M. K.; De Angelis, F.; Fantacci, S.; Selloni, A.; Viscardi, G.; Liska, P.; Ito, S.; Takeru, B.; Gratzel, M. *J. Am. Chem. Soc.* **2005**, *127*, 16835-16847.
[38]. Lundqvist, M. J.; Nilsing, M.; Persson, P.; Lunell, S. *Int. J. Quan. Chem.* **2006**, *106*, 3214-3234.
[39]. Waston, D. F.; Meyer, G. J. *Annu. Rev. Phys. Chem*. **2005**, *56*, 119-156.
[40]. Merrick, J. P.; Moran, D.; Radom, L. *J. Phys. Chem. A* **2007***, 111,* 11683-11700.
[41]. Sinha, P.; Boesch, S. E.; Gu, C.; Wheeler, R. A.; Wilson, A. K. *J. Phys. Chem. A* **2004***, 108,* 9213-9217.
[42]. Zhang, C. R.; Chen, H. S.; Wang, G. H.; *Chem. Res. Chin. U*, **2004**, *20*, 640-646.
[43]. Sun, Y.; Chen, X.; Sun, L.; Guo, X.; Lu, W. *Chem. Phys. Lett*. **2003**, *381*, 397-403.
[44]. Christiansen, O.; Gauss, J.; Stanton, J. F. *Chem. Phys. Lett.* **1999**, *305*, 147-155.
[45]. Wang, Z. S.; Huang, Y. Y.; Huang, C. H.; Zheng, J.; Cheng, H. M.;Tian, S. J. *Synth. Met*. **2000,** *14*, 201-207.
[46]. Zhang, C. R.; Wu, Y. Z.; Chen, Y. H.; Chen, H. S. *Acta Phys. Chim. Sin*. **2009**, *25*, 53-60.
[47]. Seidl, A.; Gorling, A.; Vogl, P.; Majewski, J. A.; Levy, M. *Phys. Rev. B* **1996**, *53*, 3764-3774.
[48]. Hara, K.; Sato, T.; Katoh, R.; Furube, A.; Ohga, Y.; Shinpo, A.; Suga, S.; Sayama, K.; Sugihara, H.; Arakawa, H. *J. Phys. Chem. B* **2003**, *107*, 597-606.
[49]. Zhang, C. R.; Liu, Z. J.; Chen, Y. H.; Chen, H. S.; Wu, Y. Z.; Yuan, L. H. *J. Mol. Struct.* **2009**, *899*, 86-93.